JOURNAL OF MATERIALS SCIENCE 28 (1993) 1257–1263

Enhanced ionic conduction in PbI_2–Al_2O_3 composite solid electrolytes

A. KUMAR, K. SHAHI
Materials Science Programme, Indian Institute of Technology, Kanpur 208 016, India

The PbI_2–Al_2O_3 composite solid electrolytes have been investigated by means of complex impedance analysis, X-ray diffraction, differential thermal analysis and SEM techniques. The composites prepared by solid-state reaction (method I) at a temperature (320 °C) lower than the melting point (T_m) of PbI_2 exhibit enhancement in conductivity, while those prepared by melting the mixture (method II) show a decrease in the conductivity. The enhancement in the conductivity as a function of composition (mol % of Al_2O_3 in PbI_2) and the particle size of Al_2O_3 are satisfactorily explained on the basis of a random resistor network (RRN) model which presumes the formation of a highly conducting interface layer along the matrix–particle interface. The scanning electron micrographs show that the high-conductivity interface layers do not form a connected path throughout the matrix when the concentration of the dispersoid (Al_2O_3) is small. At about 30 mol % Al_2O_3, the high-conductivity pathways are formed throughout the matrix which results in a marked enhancement in the conductivity. The RRN model appears to be valid for the PbI_2–Al_2O_3 system prepared by method I. The lowering in the conductivity of samples prepared by method II is probably due to chemical changes occurring in PbI_2–Al_2O_3 during the preparation at $T \geq T_m$ of PbI_2.

1. Introduction

The dispersion of submicrometre insulating particles such as Al_2O_3, SiO_2, ZrO_2, CeO_2, Fe_2O_3 etc. is a well known [1–10] technique to increase the ionic conductivity of several modest ionic conductors. Some of these two-phase or multi-phase composite solid electrolytes have shown promise for battery, fuel cell and sensor applications. It should however be pointed out that there are a few composite systems which show no enhancement, or even a decrease in the ionic conductivity, due to dispersion of insoluble second-phase particles [11–13].

A number of models [14–23] have been proposed to explain the seemingly unusual behaviour of enhanced conductivity due to dispersion of insoluble particles. Almost all models presume the formation of a highly conducting space-charge layer along the matrix–insulator interface and explain the observed behaviour to a varying degree of success. The random resistor network (RRN) model [18–20] appears to be the most satisfactory one as it explains not only the enhancement in σ but also the effect of particle size on σ enhancement and the subsequent decrease in the conductivity when the concentration of the dispersoid becomes large. However, as none of these models is found to be completely satisfactory, alternative possible mechanisms of σ enhancement involving a matrix phenomenon such as increased conduction along the grain boundaries and dislocations [21], the presence of a metastable phase [21] and homogeneous doping of the matrix [22] have been proposed for a variety of systems.

This paper reports the preparation of PbI_2–Al_2O_3 composite solid electrolytes and their electrical characterization by means of complex impedance analysis and phase studies by differential thermal analysis (DTA) and SEM techniques.

2. Experimental procedure

High-purity PbI_2 was obtained from Alfa Products and deagglomerated Al_2O_3 powder of three different particle sizes (0.05, 0.3 and 1.0 μm) was obtained from Buehler Micropolish II (USA). PbI_2–Al_2O_3 of various compositions was prepared in two different ways. In the method I the appropriate amounts of PbI_2 and Al_2O_3 were mixed and milled thoroughly in an acetone medium in a ball mill (Fritsch Pulverisette Type .05 .202, Germany) for 6–8 h. The powder so obtained was reground in a pestle and mortar and finally pelletized in a 9 mm diameter steel die at a pressure of 5 ton cm^{-2}. The pellets were subsequently heated at 320 °C, i.e. well below the melting point (402 °C) of PbI_2, for several hours before using them for electrical and structural studies. In method II the appropriate amounts of PbI_2 and Al_2O_3 were mixed thoroughly in a ball mill in an acetone medium and the mixture was heated at ~450 °C, i.e. above the melting point of PbI_2, for several hours to ensure a homogeneous dispersion of Al_2O_3 particles in the PbI_2 matrix, followed by cooling in the furnace, regrinding and pelletization as before. The samples prepared by both the methods were annealed at 320 °C for ~ 24 h before using them for impedance analysis, X-ray diffrac-

0022–2461 © *1993 Chapman & Hall*

tion and SEM studies. A pair of stainless steel discs (dia. 10 mm) were used as electrodes for electrical measurements.

The impedance measurements were carried out using an HP-4192A impedance analyser. The measurements were made from 320 °C to room temperature during the cooling cycle at a step of 20–25 °C. Sufficient time (1–2 h) was allowed at each temperature for thermal equilibration. The temperature of the sample was controlled within a range of ± 1 °C by using a PID temperature controller (Indotherm model 401-D). The X-ray diffraction patterns were recorded at room temperature by using a Rich Seifert (Iso-Debyeflex 2002D) counter diffractometer employing CuK_α radiation. The DTA measurements were carried out using a mini DTA apparatus (Linseis, model L62) with a heating/cooling rate of 5 °C min^{-1}. The SEM studies were carried out using a Jeol model JSM-840A scanning electron microscope to examine the distribution of Al_2O_3 particles in the PbI_2 matrix.

In addition the true stress versus true strain behaviour was investigated using an Instron 1195. The crosshead speed was kept at 0.5 mm min^{-1}.

3. Results and discussion

3.1. Complex impedance analysis

The d.c. electrical conductivities of PbI_2 and PbI_2–Al_2O_3 composites were obtained at each temperature from complex impedance analysis. The complex impedance data, i.e. the modulus of impedance $|Z|$ and the phase angle θ, were obtained over a wide frequency range (5 Hz–13 Hz). To analyse the a.c. impedance data $|Z|$ and θ an integrated software package developed in our own laboratory [24] was used which also provides for automatic data entry, acquisition and analysis. Fig. 1 shows a plot of the real part of the impedance ($Z\cos\theta$) versus the imaginary part ($Z\sin\theta$) of the impedance for PbI_2. The curves are semicircles as expected, which suggest that the electrode/electrolyte/electrode cell assembly is equivalent to a parallel combination of a pure resistor and a capacitor. Thus the diameter of the semicircular plot yields the d.c. resistance of the sample which was used to calculate the conductivity of the samples. The d.c. conductivity σ of all samples investigated in this work, namely PbI_2 and PbI_2–Al_2O_3 composites, was determined in this manner at various temperatures.

3.2. Electrical conductivity

PbI_2–Al_2O_3 composites prepared by method II showed a decrease in the conductivity over that of pure PbI_2 (Fig. 2). The lowering of the conductivity is probably due to decomposition of PbI_2 during the preparation of PbI_2–Al_2O_3 composite when it was heated above the melting point of PbI_2. The X-ray diffractograms showed that chemical changes did indeed occur in the composite prepared by method II. It was further supported by colour changes of the samples. These samples were not studied in further detail.

3.2.1. Electrical conductivity versus composition

Fig. 3 shows the variation of electrical conductivity as a function of concentration (mol %) of Al_2O_3 in PbI_2 at three different temperatures, namely 100, 250 and 150 °C. It is observed that the conductivity increases only slightly (up to 10 mol % Al_2O_3) but it rises rather rapidly subsequently and exhibits a maximum value at ~35 mol % Al_2O_3. As the concentration of Al_2O_3 increases further, the conductivity decreases rapidly and attains values even lower than that of pure PbI_2. Table I compares the properties of PbI_2–Al_2O_3 composites with those of others. These results would suggest that the conductivity of the PbI_2–Al_2O_3 system is only modestly enhanced (by a factor of ~25).

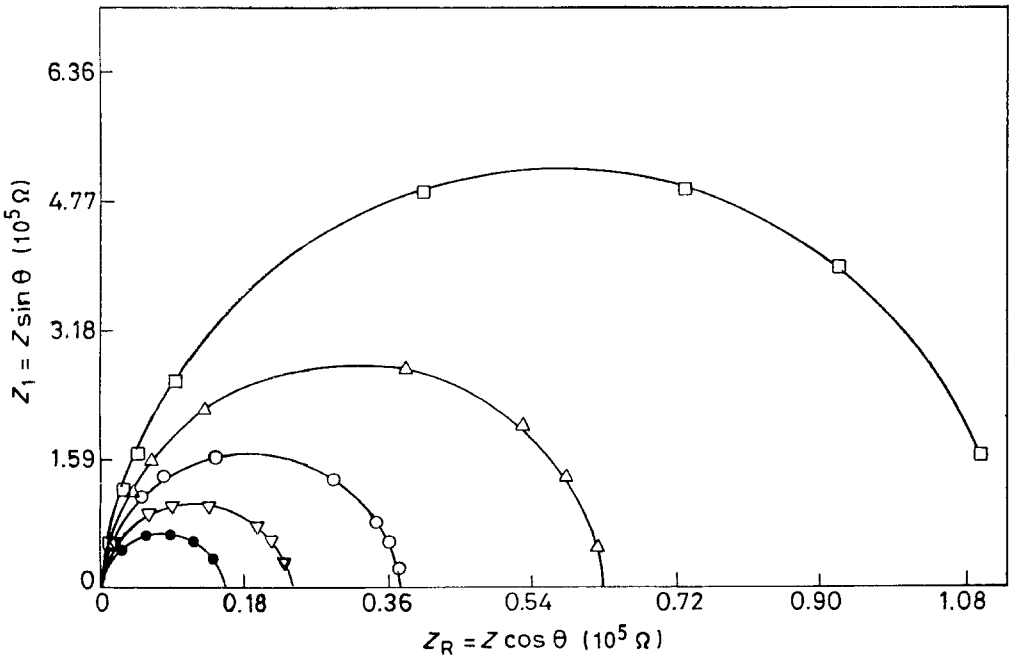

Figure 1 Complex impedance plots for pure PbI_2 at different temperatures: (□) 169 °C, (△) 191 °C, (○) 212 °C, (▽) 234 °C, (●) 256 °C.

TABLE I Composition, particle size of dispersoid and maximum enhancement in conductivity for various composite solid electrolytes, including the present PbI_2–Al_2O_3 system

Composite (host/dispersoid)	Concentration of dispersoid for maximum enhancement in σ (mol %)	Particle size (μm)	Factor of maximum enhancement in σ at (T °C)	Density (host/dispersoid)	Reference
LiI/Al_2O_3	33–45	–	10^2 (25 °C)	4.076/3.965	[1]
AgI/Al_2O_3	30	0.06	10^3 (25 °C)	5.863/3.965	[2]
$CuCl/Al_2O_3$	10	0.06	10 (25 °C)	4.14/3.965	[5]
PbI_2/Al_2O_3	~35	0.05	~25 (100 °C)	6.16/3.965	This work
CaF_2/Al_2O_3	4	0.02	10^2 (372 °C)	3.18/3.965	[8]
CaF_2/CeO_2	2–4	0.01	10^3 (372 °C)	3.18/7.132	[8]
PbF_2/ZrO_2	7.5	0.2	1.7 (25 °C)	8.24/5.89	[10]
PbF_2/Al_2O_3	7.5	0.2	1.25 (25 °C)	8.24/3.965	[10]
$LiBr \cdot H_2O/Al_2O_3$	50	8.0 ($200\ m^2\ g^{-1}$)	10 (< 307 °C)	~ 3.5/3.965	[13]

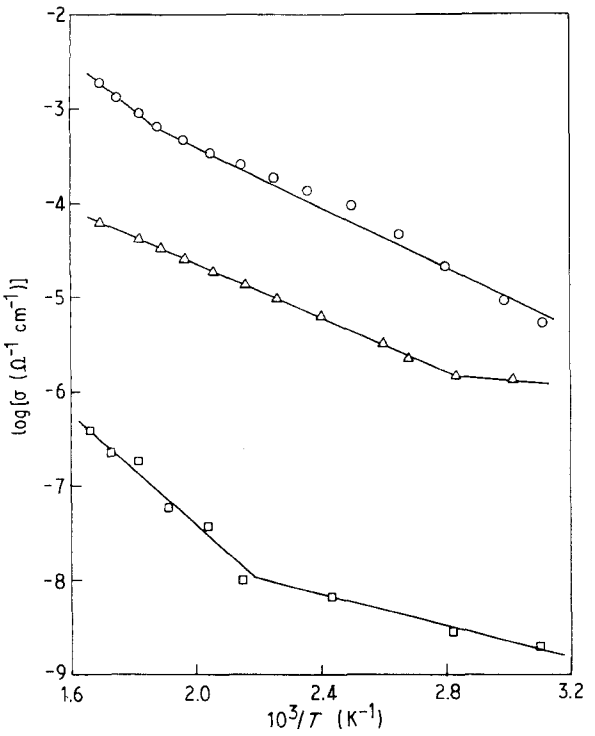

Figure 2 Logarithm of conductivity as a function of inverse temperature for (△) pure PbI_2 and for PbI_2–30 mol % Al_2O_3 prepared by (○) method I and (□) method II.

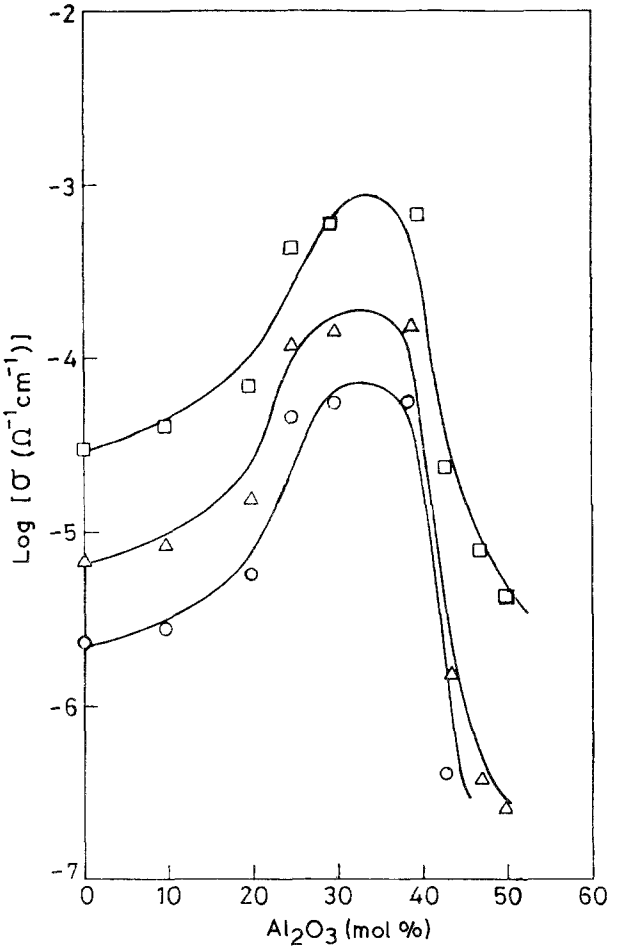

Figure 3 Electrical conductivity as a function of composition (mol % of Al_2O_3 in PbI_2) at different temperatures: (○) 100 °C, (△) 150 °C, (□) 250 °C.

However, this should be regarded as significant, especially in view of the results on PbF_2–ZrO_2 composites which exhibit almost no enhancement in the conductivity [10]. Similarly, $PbCl_2$–Al_2O_3 composites are found [11] to have a lower conductivity than that of pure $PbCl_2$. Thus the behaviour of PbI_2–Al_2O_3 appears distinctly different from those of PbF_2- and $PbCl_2$-based composites. In order to understand the mechanism of enhancement, it would appear desirable to investigate the PbF_2–Al_2O_3 and PbI_2–ZrO_2 composite systems.

As for the concentration of the dispersoid for maximum σ enhancement, there does not seem to be a definite correlation between the densities of the host and the dispersoid. While the maximum enhancement occurs around 30–45 mol% of dispersoid in the case of lithium [1, 13] and silver [2] salts, it is only ~10 mol % in the case of CuCl [5]. In the present PbI_2–Al_2O_3 system the maximum enhancement is obtained at ~35 mol % Al_2O_3 which is close to the values for silver and lithium salts, even though the former (PbI_2) is much denser than the latter.

However, if the density of the dispersoid material exceeds by far that of the host matrix, as for example in CaF_2–CeO_2 (< 0.01 μm), and if the maximum σ

still occurs at a very small concentration (2–4 mol %) of the dispersoid, it can be surmised that this concentration will not be able to form a connected high-conductivity path through the host material, thereby virtually ruling out the possibility of a space-charge layer formation mechanism. In such cases the dominant σ enhancement mechanism is probably aliovalent doping of the host matrix by the dispersoid phase.

The fact that the PbI_2–Al_2O_3 composites exhibits a maximum conductivity at ~35 mol % Al_2O_3 would suggest that space-charge layer formation is probably responsible for the enhancement. The conductivity rises rapidly when some sort of high-conductivity channel forms through the conductor. It could be either a highly conducting phase formation along the interface or space-charge layer formation along the interface. X-ray diffraction studies rule out the solubility of Al_2O_3 in PbI_2 below 320 °C, so the former mechanism does not appear to contribute to the conductivity enhancement. The results obtained are consistent with a random resistor network [18, 19] which involves the formation of a high-conductivity space-charge layer along the normal conductor–insulator interface. The scanning electron micrographs show that Al_2O_3 particles are uniformly distributed in the PbI_2 matrix but the PbI_2–Al_2O_3 interface does not form a connected path throughout the sample. For 30 mol % Al_2O_3–PbI_2 composite, however, the micrographs show that Al_2O_3 particles are so distributed in the PbI_2 matrix that the interface between them appears to form connectivity throughout the sample. At still higher concentration (> 40 mol % of Al_2O_3) the connected pathways get disrupted as they begin to form closed loops due to the increased concentration of insulating bonds [20]. This results in a drastic decrease in the conductivity.

It has been reported previously that the magnitude of enhancement in conductivity depends upon the morphology or the surface activity [5, 10], shape [13] and size [3, 5] of the insulating phase particles. To observe the effect of surface activity, the Al_2O_3 particles were treated with a basic medium (NaOH solution, pH = 9.6) and it was found that the treated particles were almost twice as effective in enhancing the conductivity as the untreated Al_2O_3 particles. Table II summarizes the normalized conductivity of PbI_2–30 mol % Al_2O (as received) and PbI_2–30 mol % Al_2O_3 (NaOH treated) at three different temperatures: 100, 150 and 250 °C. The increased effectiveness of NaOH-treated Al_2O_3 particles may be due to increased interaction between the surface of the dispersed particle and the mobile anions, resulting in widening of the space-charge layer along the interface causing more enhancement in the conductivity. This leads us to conclude that surface chemistry plays a dominant role in the observed conductivity enhancement. Further studies involving dispersion of insulating particles treated with solutions of varying pH values are being planned and will be reported later.

TABLE II Normalized conductivity[a] of PbI_2–30 mol % Al_2O_3 (as received) and PbI_2–30 mol % Al_2O_3 (NaOH treated, pH = 9.6) at three different temperatures

Sample	σ^{30}/σ^0		
	100 °C	150 °C	250 °C
As received	23.5	20.86	19.04
NaOH treated	49.15	48.9	46.99

[a]Where σ^{30}/σ^0 is the ratio of conductivity of PbI_2–30 mol % Al_2O_3 to that of pure PbI_2.

3.2.2. Electrical conductivity versus particle size

Fig. 4 shows the variation of logarithm of conductivity of PbI_2–30 mol % Al_2O_3 composite solid electrolyte versus the logarithm of the particle size of Al_2O_3 particles at different temperatures. It is evident that as the particle size of the dispersoid increases the relative enhancement in the conductivity σ decreases rather drastically initially but tends to level off at larger particle sizes. Table III compares the normalized conductivity of the PbI_2–30 mol % Al_2O_3 composite

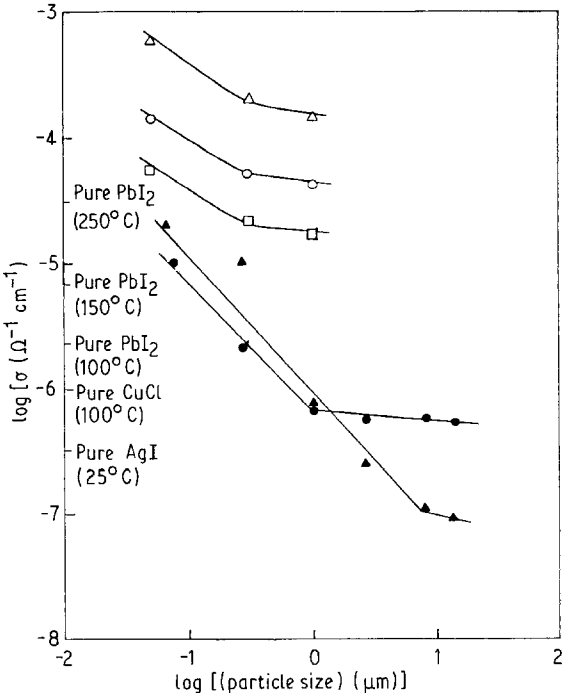

Figure 4 Logarithm of conductivity as a function of particle size of dispersoid for (●) AgI–30 mol % Al_2O_3 at 25 °C; (▲) CuCl–10 mol % Al_2O_3 at 100 °C; and PbI_2–30 mol % Al_2O_3 at (□) 100 °C, (○) 150 °C and (△) 250 °C.

TABLE III Normalized conductivity[a] of PbI_2–30 mol % Al_2O_3 for different particle sizes of Al_2O_3 (0.05, 0.3 and 1.0 μm) at three different temperatures

Particle size (μm)	σ^{30}/σ^0		
	100 °C	150 °C	250 °C
0.05	23.5	20.86	19.04
0.3	8.93	7.77	6.46
1.0	7.1	5.89	4.47

[a] Where σ^{30}/σ^0 is the ratio of conductivity of PbI_2–30 mol % Al_2O_3 to that of pure PbI_2.

system for three different particles sizes (0.05, 0.3 and 1.0 μm) at three different temperatures (100, 150 and 250 °C). The table shows that the relative enhancement in conductivity is higher for lower particle sizes of Al_2O_3. These results are comparable to the results reported previously [3–5] on a variety of systems. Many models [14–16] have since been presented to explain the observed dependence of enhancement in conductivity on the particle size. These models describe, rather empirically, the conductivity enhancement as a function of the inverse of radius of the dispersed particles. However, recent studies have emphasized the correlation of increase in the conductivity with the increase in the effective surface area of the dispersed phase [13]. The RRN model [20] qualitatively explains the observed results. For larger particles, the surface area per unit volume available for forming highly conducting bonds will be smaller, causing less enhancement in the conductivity than that for smaller particle sizes.

3.2.3. Electrical conductivity versus temperature

The d.c. electrical conductivity σ of PbI_2 and various PbI_2–Al_2O_3 composites as a function of inverse temperature is shown in Fig. 5. The log σ versus $1/T$ behaviour is of Arrhenius type for all the compositions. The transport parameters, namely the pre-exponential factor σ_0 and the activation energy E_a, are given in Table IV. The dependence of activation energy on the composition is discussed in the next section. It is evident from the results shown in Fig. 5 and from the data presented in Table IV that the effect of dispersion is to slightly decrease the activation energy. These results suggest that the concentration of defects increases at the PbI_2–Al_2O_3 interface due to the dispersion. As XRD results rule out the possibility of solubility of Al_2O_3 in PbI_2, especially at lower temperatures, these excess defects cannot be attributed to aliovalent doping. Therefore the only possibility is that of space-charge layer formation along the PbI_2–Al_2O_3 interface. These results are consistent with the results reported earlier [4–8] for various other composite systems.

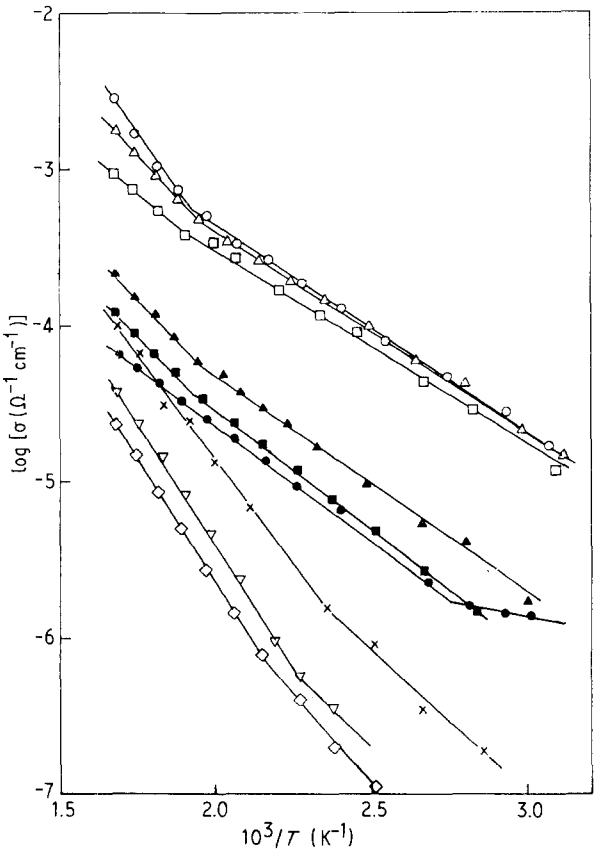

Figure 5 Logarithm of conductivity as a function of inverse temperature for PbI_2–x mol % Al_2O_3 as-received composites: x = (●) 0, (■) 10, (▲) 20, (□) 25, (△) 30, (○) 40, (×) 43, (▽) 47, (◇) 50.

Fig. 6 compares the log σ versus $10^3/T$ plots for PbI_2–30 mol % Al_2O_3 (as received) and PbI_2–30 mol % Al_2O_3 (NaOH treated, pH = 9.6). The base-treated Al_2O_3 particles produce a higher conductivity enhancement. This result has been discussed in section 3.2.1.

Fig. 7 shows the log σ versus $10^3/T$ plots for PbI_2–30 mol % Al_2O_3 for three different particle sizes of Al_2O_3, namely 0.05, 0.3 and 1.0 μm. As expected, the enhancement in the conductivity is higher for lower particle sizes of Al_2O_3, and the log σ versus $1/T$ plots are linear. The activation energies and the pre-exponential factors are listed in Table V. It is observed that the activation energy is almost independent of the particle size though the pre-exponential factor decreases as the particle size increases.

3.2.4. Activation energy versus composition

Fig. 8 shows the variation of activation energy E_a (eV) as a function of concentration of Al_2O_3 in PbI_2 ($T \leq 150$ °C). This result is consistent with the generally observed relation for ionic conductors, that the increase in conductivity is almost invariably associated with a decrease in activation energy. The figure shows that the activation energy initially decreases as the concentration of Al_2O_3 in PbI_2 increases up to about 25 mol % of Al_2O_3, when the conduction pathways just form connectivity throughout the solid. The activation energy remains almost constant in the composition range 25–40 mol % wherein the connected

TABLE IV Ionic transport parameters: the pre-exponential factors and activation energy of PbI_2–Al_2O_3 composites

Concentration of Al_2O_3 in PbI_2 (mol %)	Temperature range (°C)	E_a (eV)	σ_0 Ω^{-1} cm^{-1}
0	100–300	0.29	1.92×10^{-2}
10	100–250	0.31	4.08×10^{-2}
20	100–225	0.28	3.26×10^{-2}
25	100–225	0.25	1.09×10^{-1}
30	100–225	0.26	1.72×10^{-1}
40	100–225	0.26	1.88×10^{-1}
43	100–150	0.36	3.14×10^{-2}
	175–300	0.53	3.08×10^{-2}
47	125–175	0.44	6.57×10^{-2}
	200–300	0.57	2.39×10^{-2}
50	125–175	0.46	7.87×10^{-2}
	200–300	0.64	6.35×10^{-2}

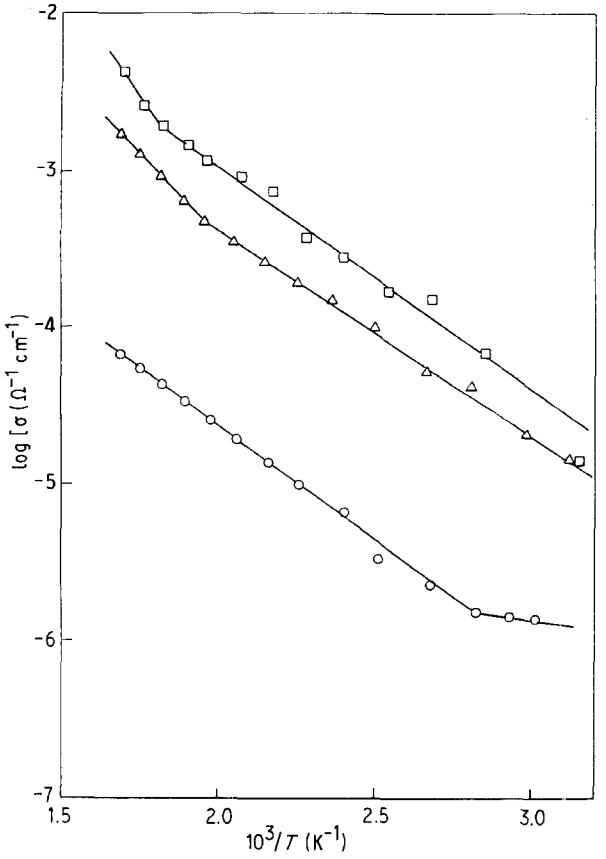

Figure 6 Logarithm of conductivity as a function of inverse temperature for (○) pure PbI_2 and for PbI_2–30 mol % Al_2O_3 composite having Al_2O_3 (△) as received and (□) treated with NaOH (pH = 9.6).

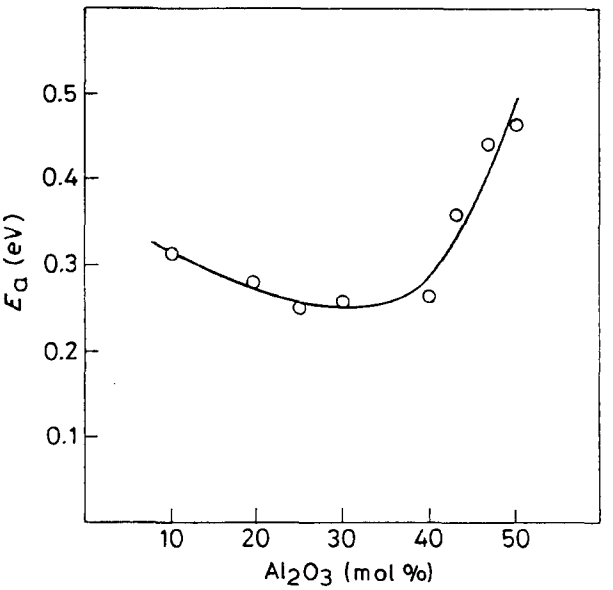

Figure 8 Activation energy versus concentration of Al_2O_3 in PbI_2 below 150 °C.

TABLE V Ionic transport parameters: the pre-exponential factor and activation energy for PbI_2–30 mol % Al_2O_3 for three different particle sizes of Al_2O_3 in the temperature range 100–200 °C

Particle size (μm)	E_a (eV)	σ_0 (Ω^{-1} cm^{-1})
0.05	0.26	1.72×10^{-1}
0.3	0.25	4.97×10^{-2}
1.0	0.24	2.86×10^{-2}

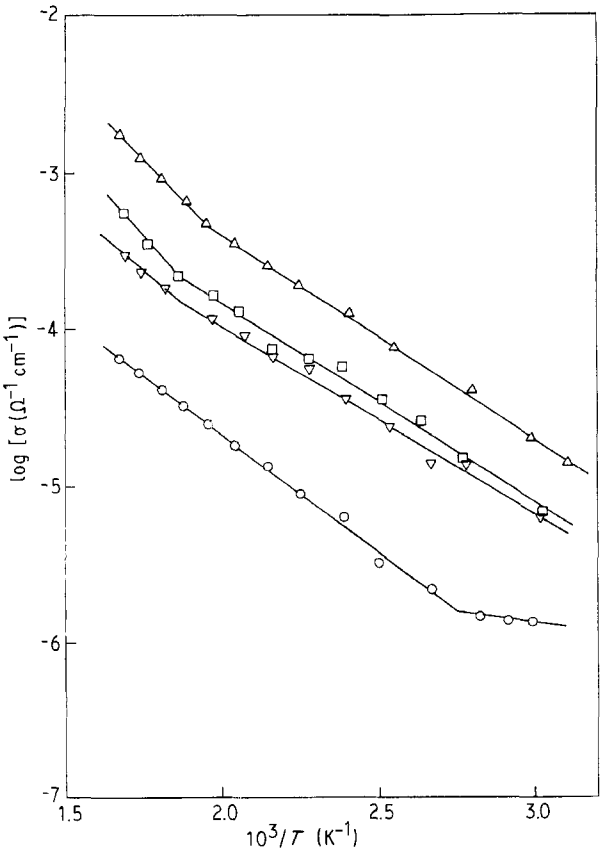

Figure 7 Logarithm of conductivity as a function of inverse temperature for (○) pure PbI_2 and PbI_2–30 mol % Al_2O_3 composite for different Al_2O_3 particle sizes: (△) 0.05 μm, (□) 0.3 μm, (▽) 1.0 μm.

TABLE VI Maximum tensile strength and Young's modulus for PbI_2–Al_2O_3 composite systems at room temperature

Composition	Maximum tensile strength (N m^{-2})	Young's modulus (N m^{-2})
PbI_2	1.5×10^4	2.03×10^6
PbI_2–30 mol % Al_2O_3	1.55×10^4	2.98×10^6
PbI_2–50 mol % Al_2O_3	3.15×10^4	5.08×10^6

paths remain formed. For concentration higher than 40 mol % the activation energy increases sharply. This concentration region is also associated with a drastic drop (see Fig. 3) in the electrical conductivity wherein the highly conducting paths get disrupted. The constant activation energy region in the composition (25–40 mol %) can be used to infer the concentration region wherein the highly conducting paths remain formed. At concentrations lower than 25 mol % the formation of highly conducting pathways is not complete, and at concentration higher than 40 mol % the conducting pathways get disrupted due to excessive formation of non-conducting bonds [20].

3.3. True stress versus true strain

In order to examine the effect of dispersion on the mechanical properties of the composites, true stress versus true strain was studied for PbI_2, PbI_2–

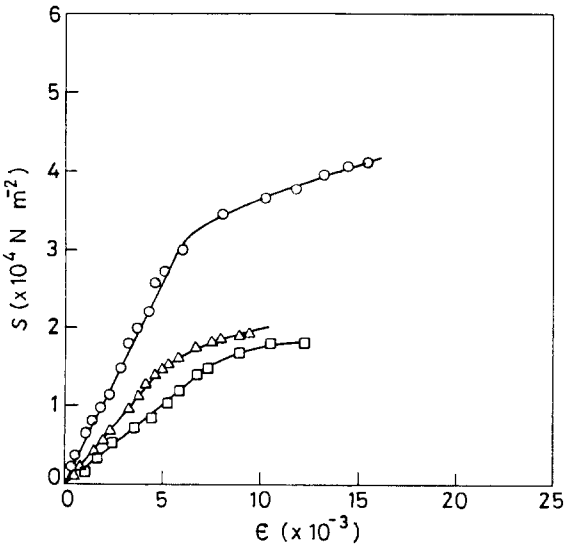

Figure 9 True stress as a function of true strain for (□) PbI_2, (△) PbI_2–30 mol % Al_2O_3 and (○) PbI_2–50 mol % Al_2O_3.

30 mol % Al_2O_3 and PbI_2–50 mol % Al_2O_3 systems. The results are shown in Fig. 9. Table VI summarizes the maximum tensile strength and Young's modulus for these compositions. Both these show a small improvement with the dispersion of 30 mol % Al_2O_3. However, the sample containing 50 mol % Al_2O_3 shows a marked improvement in the mechanical properties but as discussed earlier, its conductivity is too low. The improved mechanical properties of 50 mol % PbI_2–Al_2O_3 composite are probably due to dispersion hardening [25], wherein fine dispersed Al_2O_3 particles produce resistance to deformation by pinning the dislocation movement. Thus it is concluded that the dispersion of Al_2O_3 in PbI_2 improves both the electrical conductivity and the mechanical strength of the composite solid electrolytes.

References

1. C. C. LIANG, *J Electrochem. Soc.* **120** (1973) 1289.
2. K. SHAHI and J. B WAGNER Jr, *ibid.* **128** (1981) 6.
3. O. NAKAMURA and J. B GOODENOUGH, *Solid State Ionics* **7** (1982) 119.
4. J. MAIER, *Mater. Res. Bull.* **20** (1985) 383.
5. M. R-W. CHANG, K. SHAHI and J. B. WAGNER Jr, *J, Electrochem. Soc.* **131** (1984) 1213.
6. J. B. WAGNER Jr, *Mater. Res. Bull.* **15** (1980) 169.
7. J. MAIER and B. REICHERT Ber Bunsenges. *Phys. Chem.* **90** (1986) 666.
8. N. VAIDEHI, R. AKILA, A. K. SHUKLA and K. T. JACOB, *Mater. Res. Bull.* **21** (1986) 909.
9. S. FIJITSU, K. KOUMOTO and H. YANAGIDA, *Solid State Ionics* **18/19** (1986) 1146.
10. A. K. SHUKLA, R. MANOHARAN and J. B. GOODENOUGH, *ibid.* **26** (1988) 5.
11. A. BRUNE and J. B. WAGNER, *ibid.* **25** (1987) 165.
12. H. YAHIRO, K. EGUCHI and H. ARAI, *ibid.* **21** (1986) 37.
13. C. T. SLADE and I. M. THOMPSON, *ibid.* **26** (1988) 287.
14. C. WAGNER, *J. Phys. Chem. Solids* **33** (1972) 1051.
15. T. JOW and J. B. WAGNER Jr, *J. Electrochem. Soc.* **126** (1979) 163.
16. A. M. STONEHAM, E. WADE and J. A. KILNER, *Mater. Res. Bull.* **14** (1979) 661.
17. J. MAIER, *Mater. Chem. Phys.* **17** (1987) 485.
18. A. BUNDE, W. DIETERICH and H. E. ROMAN, *Phys. Rev. Lett.* **55** (1985) 5.
19. H. E. ROMAN, A. BUNDE and W. DIETERICH, *Phys. Rev. B* **34** (1986) 3439.
20. H. E. ROMAN and M. YOSSOUFF, *ibid.* **36** (1987) 7285.
21. N. J. DUDNEY, *J. Amer. Ceram. Soc.* **75** (1987) 65.
22. T. L. WEN, R. A. HUGGINS, A. RABENAU and W. WEPPNER, *Rev. Chim. Min.* **20** (1983) 643.
23. S. PACK, B. OWENS and J. B. WAGNER Jr, *J. Electrochem. Soc.* **127** (1980) 2177.
24. S. BHATNAGAR, S. GUPTA and K. SHAHI, *Solid State Ionics* **31** (1988) 107.
25. J. WULFF, (ed.), "The Structure and Properties of Materials," Vol. 2 (Wiley, New York, 1966; Wiley Eastern, New Delhi, 1968) p. 179.

Received 28 October 1991
and accepted 14 August 1992